Supplementary materials

DeepMapi: A Fully Automatic Registration Method for Mesoscopic Optical Brain Images Using Convolutional Neural Networks

Hong Ni[1], Zhao Feng[1], Yue Guan[1], Xueyan Jia[2], Wu Chen[1], Tao Jiang[2], Qiuyuan Zhong[1], Jing Yuan[1, 2], Miao Ren[2, 3], Xiangning Li[1, 2], Hui Gong[1, 2, 4], Qingming Luo[1, 2, 3], Anan Li[1, 2, 4,*]

[1] *Britton Chance Center for Biomedical Photonics, Wuhan National Laboratory for Optoelectronics, MoE Key Laboratory for Biomedical Photonics, School of Engineering Sciences, Huazhong University of Science and Technology, Wuhan, China*

[2] *HUST-Suzhou Institute for Brainsmatics, JITRI Institute for Brainsmatics, Suzhou, China*

[3] *School of Biomedical Engineering, Hainan University, Haikou, China*

[4] *CAS Center for Excellence in Brain Science and Intelligence Technology, Chinese Academy of Science, Shanghai, China*

[*] Corresponding author.

E-mail: aali@mail.hust.edu.cn (Li A)

Supplementary Fig. 1: The registration results used for training and augmentation.

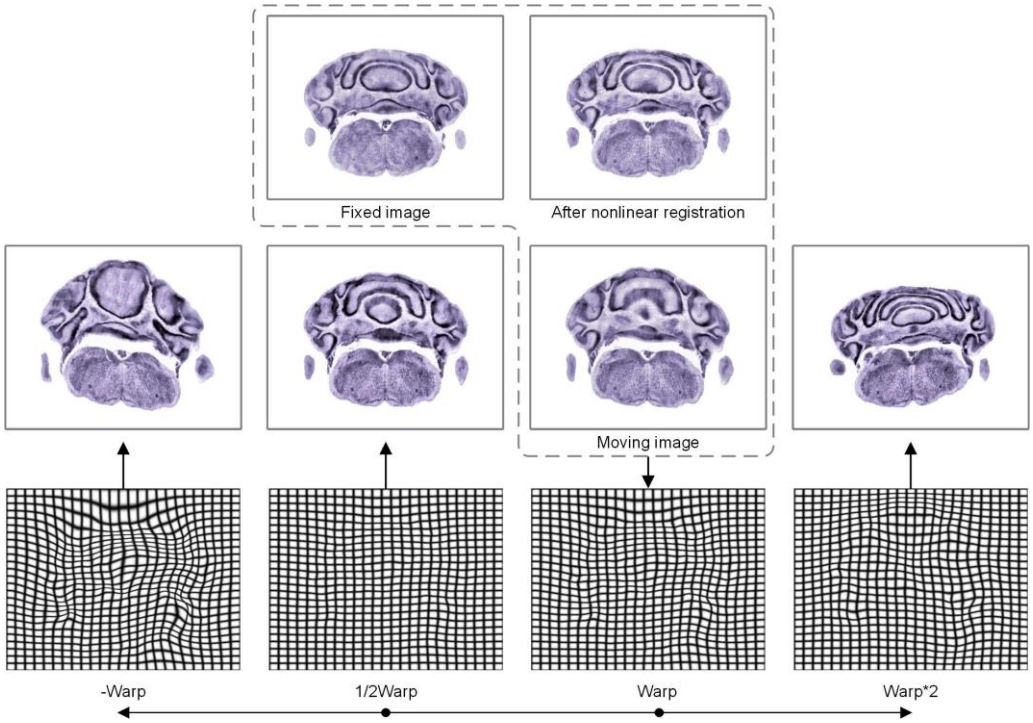

The dashed box shows the registration result for the fixed image and the corresponding deformation field (Warp, third column). The first column shows the deformation field obtained in the negative direction (-Warp) and the corresponding deformed moving image. The second column shows the deformation field obtained in the half-positive direction (1/2 Warp) and the corresponding deformation moving image. The fourth column shows the deformation field obtained in the twice position direction (2 Warp) and the corresponding deformed moving image.

Supplementary Fig. 2: The registration results of the fixed image to the standard brain atlas.

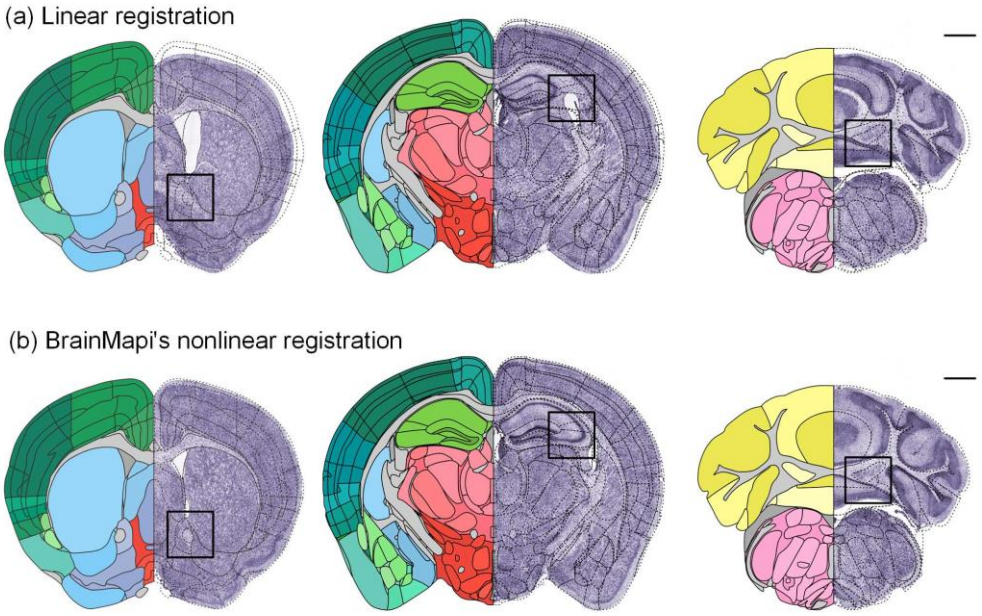

The 10 μm thick projections of three coronal sections. The left part of the images shows the Allen CCF v3, and the right part of the images shows the black dotted line of the Allen CCF v3 superimposed on the image. **(a)** The linear registration results for the Allen CCF v3 brain atlas. **(b)** The nonlinear registration results for the Allen CCF v3 brain atlas using the BrainMapi method. Scale bar: 1 mm. The region lines is from the Allen CCF v3, © 2004 Allen Institute for Brain Science. Allen Mouse Brain Atlas. Available from: atlas.brain-map.org.

Supplementary Fig. 3: The architecture of the convolutional neural network.

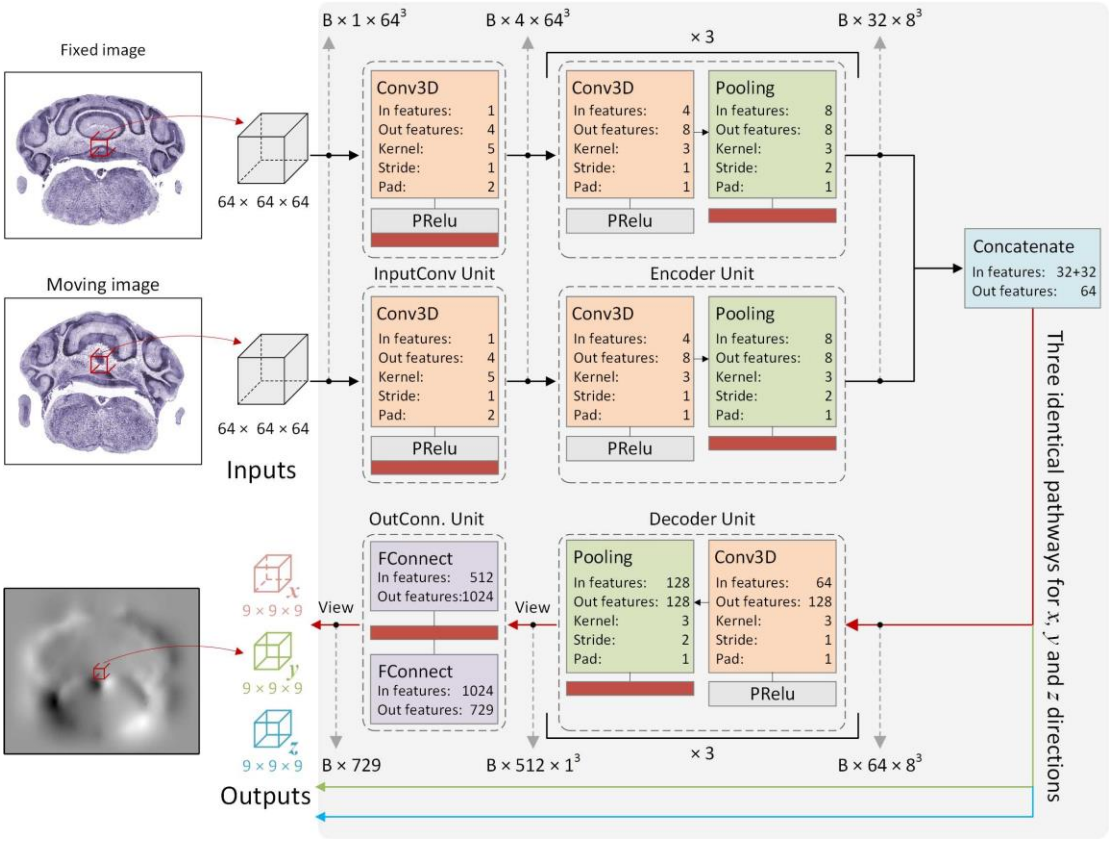

The variant patch-based network. The inputs are two 3D blocks from the fixed and moving images, respectively, and the outputs are three 3D patches corresponding to the displacement in the x, y and z directions. The network is composed of an InputConv Unit, Encoder Unit, Decoder Unit and OutConn Unit. Conv3D represents the 3D convolution layer, and Pooling indicates the pooling layer, Concatenate connects the two branches, and FConnect indicates the fully connected layer. The “kernel” represents the kernel size, “stride” indicates the step size, “pad” is the size of the edge zero padding during convolution or pooling, and B represents the batch size during training.

Supplementary Fig. 4: The quantitative assessment before and after self-feedback.

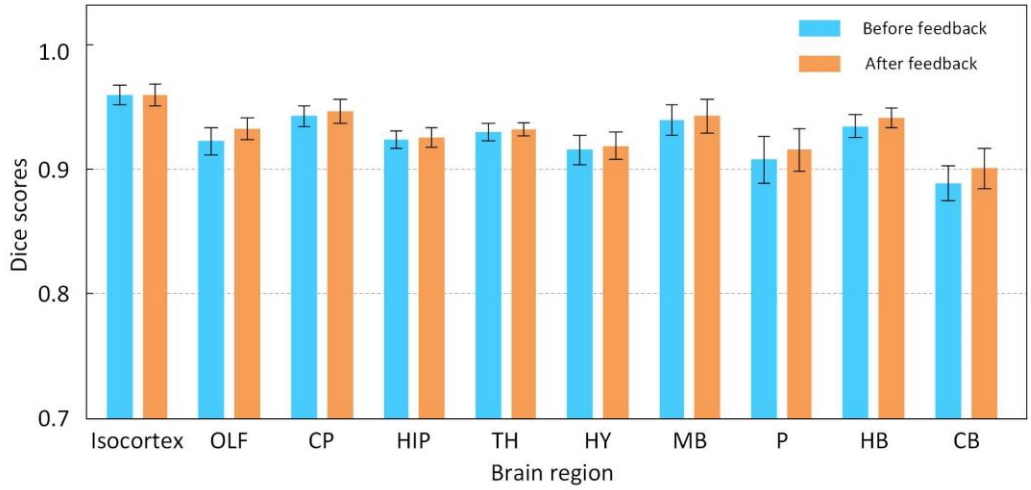

Mean Dice score comparisons of 10 brain regions before (blue) and after (orange) applying the self-feedback strategy.

Supplementary Fig. 5: The quantitative assessment of the dual-hierarchical results.

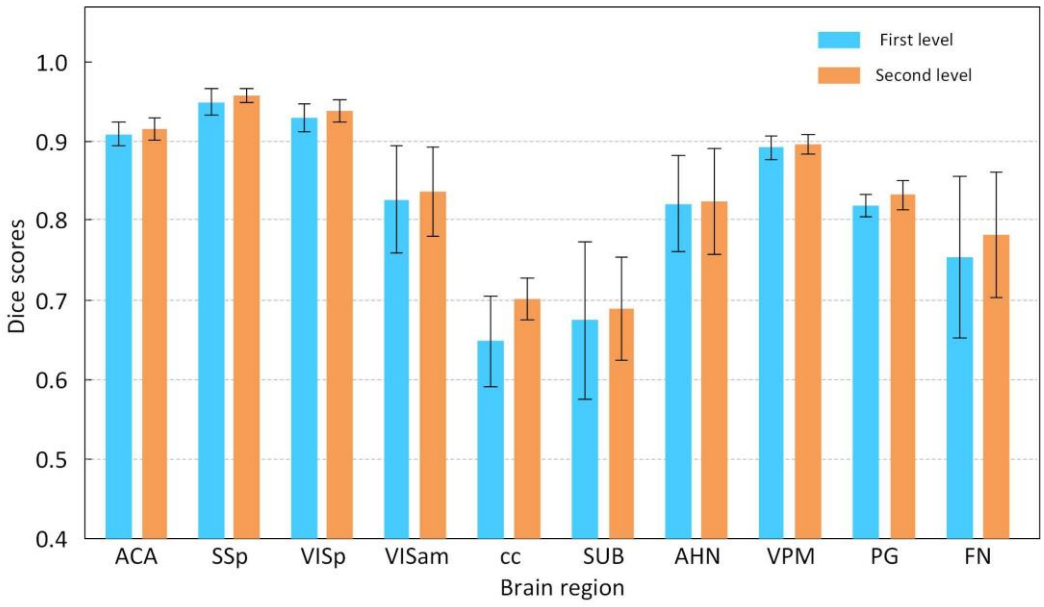

Mean Dice score comparisons of 10 smaller brain regions or nuclei in the first- and second-level.

Supplementary Fig. 6: The registration results of different unsupervised methods.

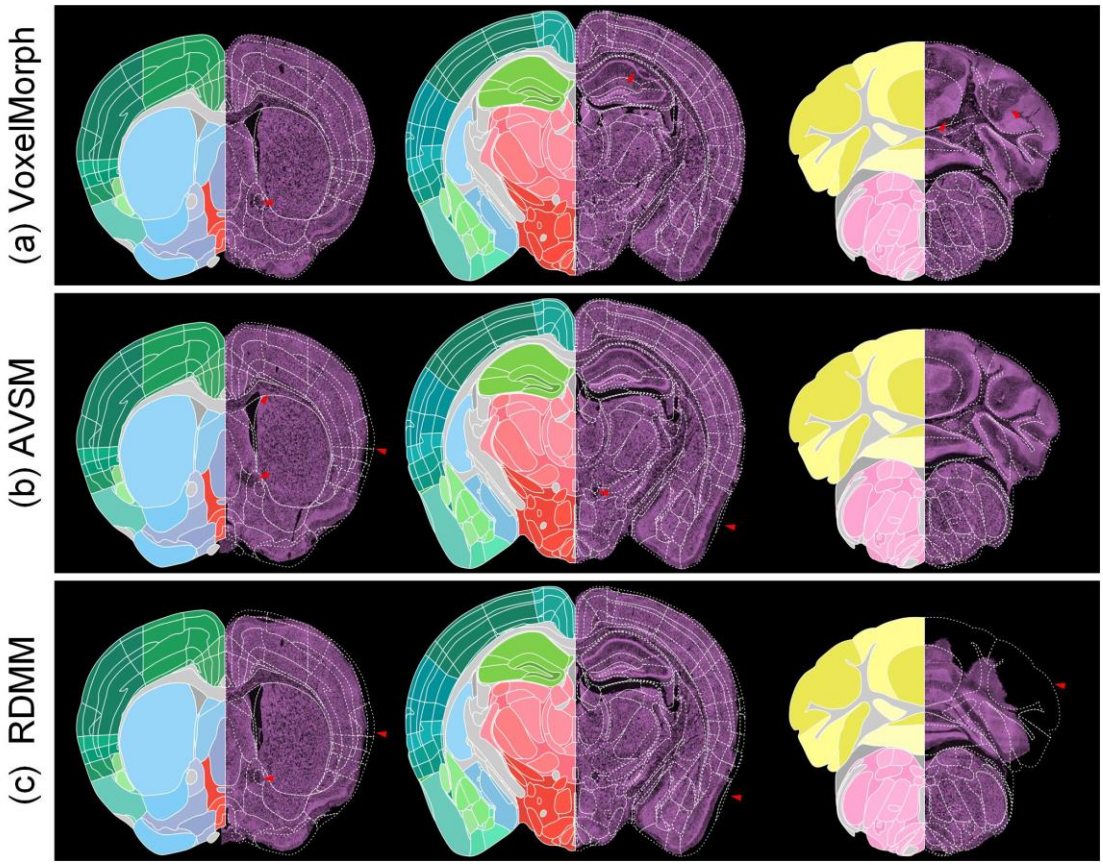

Three coronal sections. The left part of the image is the Allen CCF v3, and the right part of each image shows the white dotted line of the Allen CCF v3 superimposed on the registered image. The regions with inaccurate registration result are indicated with red arrows. **(a)** VoxelMorph. **(b)** AVSM. **(c)** RDMM. The region lines are from the Allen CCF v3, © 2004 Allen Institute for Brain Science. Allen Mouse Brain Atlas. Available from: atlas.brain-map.org.

Supplementary Fig. 7: The colormap of Jacobian of the displacement field obtained by DeepMapi method.

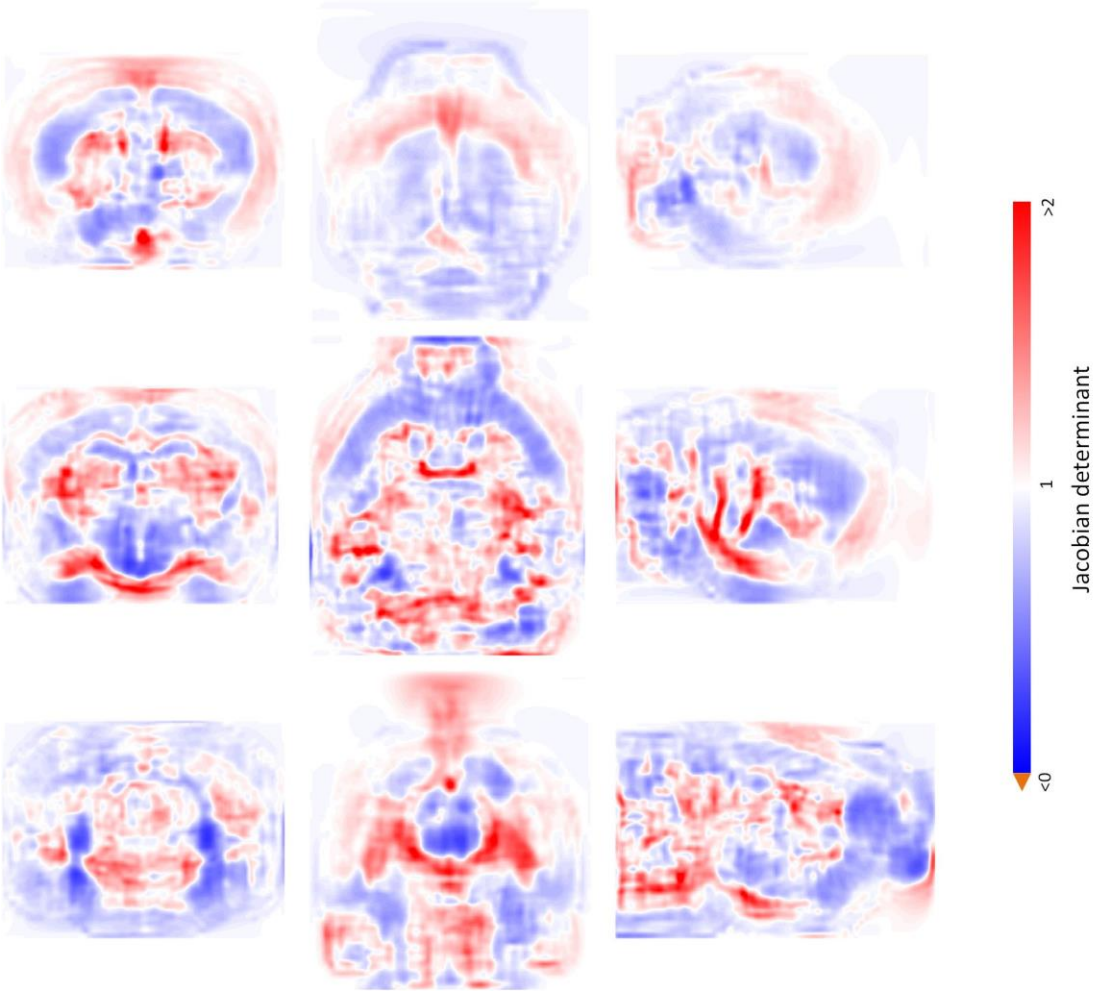

The nine anatomical sections of coronal, horizontal and sagittal, respectively. The color map of the Jacobian with singularities (folding) indicated in the brown (< 0), and as shown in the figure that there are no singularities by DeepMapi method.

Supplementary Fig. 8: The colormap of Jacobian of the displacement field for Model 1-5, before/after self-feedback and with/without dual-hierarchical.

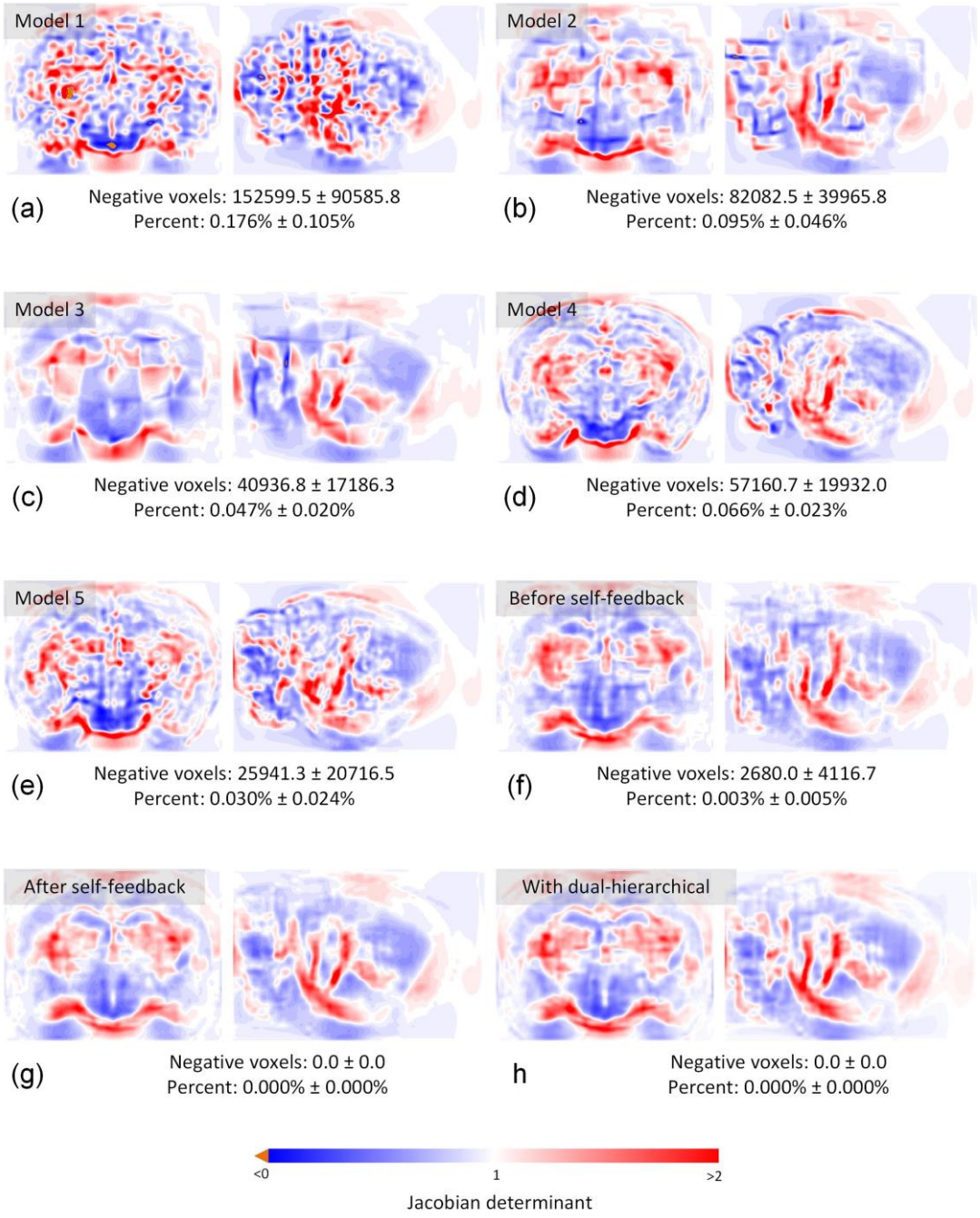

The anatomical sections of coronal and sagittal, respectively. The color map of the Jacobian with singularities (folding) indicated in the brown (< 0). **(a)** Model 1, **(b)** Model 2, **(c)** Model 3, **(d)** Model 4, **(e)** Model 5, **(f)** Before self-feedback, **(g)** After self-feedback, **(h)** With dual-hierarchical.

Supplementary Table 1 Detail training information of six models.

	Model type	Input size	Output size	First feature number	E/D Coder number	Stride	Batch size
Model 1	FCN	16	16	32	2/2	32	64
Model 2	FCN	32	32	16	3/3	32	16
Model 3	FCN	64	64	8	3/3	64	4
Model 4	Patch	16	3	32	2/2	16	64
Model 5	Patch	32	5	16	3/2	32	32
Model 6	Patch	64	9	4	3/3	32	64

Supplementary Table 2 Comparisons of six models of loss value and running time.

Test model	Train loss/3pixels	Valid loss/3pixels	Training time	Predicted time
model 1	1.35 ± 0.05	7.41 ± 0.12	5d11h3m	2m20s ± 1s
model 2	1.11 ± 0.03	5.21 ± 0.06	13d6h50m	1m34s ± 1s
model 3	1.26 ± 0.04	3.45 ± 0.08	**13d18h22m**	1m39s ± 1s
model 4	0.97 ± 0.03	6.45 ± 0.03	4d11h44m	**21m4s ± 12s**
model 5	0.97 ± 0.05	4.99 ± 0.05	2d14h45m	16m42s ± 5s
model 6	**0.62 ± 0.03**	**3.17 ± 0.04**	4d6h22m	5m46s ± 2s

Supplementary Table 3 Mean absolute and mean Dice Scores of six models and P values of Wilcoxon signed-rank test among Model 6 and other five models.

Model	Model 1	Model 2	Model 3	Model 4	Model 5	Model 6
Mean absoute values (× 10 μm)	2.490 ± 2.385	1.761 ± 1.733	1.521 ± 1.743	2.401 ± 2.208	1.861 ± 1.811	**1.350 ± 1.475**
P values	3.610e-41	8.112e-14	9.604e-04	3.078e-41	3.952e-18	—
Mean dice scores	0.885 ± 0.040	0.919 ± 0.025	0.924 ± 0.025	0.910 ± 0.031	0.915 ± 0.027	**0.927 ± 0.022**
P values	7.557e-10	4.537e-08	0.080	3.367e-09	9.068e-10	—

Supplementary Table 4 Mean Dice Scores comparisons for ten large brain regions of six models.

Structures	Mean dice scores					
	model1	model2	model3	model4	model5	model6
Isocortex	0.935 ± 0.015	0.958 ± 0.007	0.958 ± 0.011	0.953 ± 0.009	0.955 ± 0.008	**0.960 ± 0.008**
OLF	0.902 ± 0.019	0.918 ± 0.017	**0.933 ± 0.014**	0.913 ± 0.014	0.913 ± 0.012	0.923 ± 0.011
CP	0.903 ± 0.018	0.936 ± 0.013	0.939 ± 0.013	0.928 ± 0.019	0.935 ± 0.012	**0.943 ± 0.008**
HIP	0.850 ± 0.054	0.917 ± 0.014	0.914 ± 0.019	0.906 ± 0.025	0.909 ± 0.017	**0.924 ± 0.007**
TH	0.891 ± 0.023	0.917 ± 0.010	0.925 ± 0.013	0.910 ± 0.027	0.918 ± 0.015	**0.930 ± 0.007**
HY	0.861 ± 0.026	0.899 ± 0.013	0.905 ± 0.021	0.886 ± 0.031	0.889 ± 0.023	**0.916 ± 0.012**
MB	0.898 ± 0.027	0.931 ± 0.011	0.939 ± 0.009	0.924 ± 0.018	0.927 ± 0.014	**0.940 ± 0.012**
P	0.865 ± 0.029	0.899 ± 0.019	0.906 ± 0.017	0.886 ± 0.034	0.894 ± 0.026	**0.908 ± 0.019**
HB	0.912 ± 0.014	0.932 ± 0.012	**0.937 ± 0.012**	0.925 ± 0.019	0.930 ± 0.014	0.935 ± 0.009
CB	0.832 ± 0.033	0.882 ± 0.020	0.885 ± 0.017	0.874 ± 0.022	0.876 ± 0.017	**0.889 ± 0.014**

Supplementary Table 5 Mean Dice Scores for ten brain regions before and after self-feedback.

Structures	Before feedback(Dice scores)	After feedback(Dice scores)
Isocortex	0.960 ± 0.008	**0.960 ± 0.009**
OLF	0.923 ± 0.011	**0.933 ± 0.009**
CP	0.943 ± 0.008	**0.947 ± 0.010**
HIP	0.924 ± 0.007	**0.926 ± 0.008**
TH	0.930 ± 0.007	**0.933 ± 0.005**
HY	0.916 ± 0.012	**0.919 ± 0.011**
MB	0.940 ± 0.012	**0.943 ± 0.014**
P	0.908 ± 0.019	**0.916 ± 0.017**
HB	0.935 ± 0.009	**0.942 ± 0.008**
CB	0.889 ± 0.014	**0.901 ± 0.016**

Supplementary Table 6 Mean Dice Scores for ten brain regions or nucleus in the first- and second-level.

Structures	First-hierarchy (Dice scores)	Second-hierarchy (Dice scores)
ACA	0.908 ± 0.015	**0.915 ± 0.014**
SSp	0.949 ± 0.016	**0.957 ± 0.008**
VISp	0.929 ± 0.017	**0.937 ± 0.014**
VISam	0.826 ± 0.067	**0.836 ± 0.056**
cc	0.648 ± 0.057	**0.701 ± 0.026**
SUB	0.674 ± 0.099	**0.688 ± 0.065**
AHN	0.821 ± 0.061	**0.824 ± 0.067**
VPM	0.892 ± 0.015	**0.896 ± 0.012**
PG	0.819 ± 0.014	**0.832 ± 0.018**
FN	0.753 ± 0.102	**0.781 ± 0.079**

Supplementary Table 7 Mean Dice Scores for 140 brain regions or nucleus of Affine (Aff.), LD demons (LD-D.), SyN, VoxelMorph (V.M.), AVSM (AV.), RDMM (RD.), QuickSilver (Q.S.), VNet (VN.) and DeepMapi (D.M.) methods.

No.	Brain regions	Brain region full name	Traditional method			Unsupervised method			Supervised method		
			Aff.	LD-D.	SyN	V.M.	AV.	RD.	Q.S.	VN.	D.M.
1	MOs	Secondary motor area	0.695	0.796	0.910	0.878	0.659	0.823	0.894	0.902	0.932
2	MOp	Primary motor area	0.741	0.759	0.922	0.905	0.658	0.852	0.920	0.917	0.943
3	AId	Agranular insular area, dorsal part	0.673	0.644	0.841	0.825	0.611	0.633	0.873	0.897	0.915
4	AIv	Agranular insular area, ventral part	0.636	0.553	0.763	0.787	0.626	0.616	0.841	0.878	0.887
5	AIp	Agranular insular area, posterior part	0.683	0.662	0.848	0.858	0.746	0.776	0.895	0.882	0.922
6	ORBl	Orbital area, lateral part	0.545	0.658	0.814	0.748	0.391	0.602	0.793	0.861	0.871
7	ORBm	Orbital area, medial part	0.375	0.591	0.761	0.644	0.126	0.417	0.729	0.802	0.719
8	ORBvl	Orbital area, ventrolateral part	0.456	0.560	0.802	0.668	0.183	0.490	0.724	0.813	0.768
9	ACAv	Anterior cingulate area, ventral part	0.544	0.753	0.880	0.796	0.661	0.787	0.780	0.806	0.875
10	ACAd	Anterior cingulate area, dorsal part	0.619	0.640	0.849	0.749	0.654	0.734	0.784	0.823	0.884
11	PL	Prelimbic area	0.547	0.696	0.852	0.760	0.334	0.676	0.803	0.838	0.866
12	ILA	Infralimbic area	0.081	0.586	0.822	0.643	0.212	0.509	0.706	0.748	0.769
13	GU	Gustatory areas	0.674	0.519	0.844	0.848	0.676	0.647	0.895	0.882	0.933
14	SSp	Primary somatosensory area	0.812	0.883	0.942	0.933	0.837	0.898	0.939	0.938	0.960
15	SSs	Supplemental somatosensory area	0.787	0.803	0.906	0.903	0.772	0.817	0.933	0.927	0.951
16	VISC	Visceral area	0.728	0.638	0.833	0.849	0.693	0.722	0.891	0.859	0.916
17	AUDd	Dorsal auditory area	0.721	0.473	0.720	0.779	0.505	0.698	0.853	0.833	0.901

18	AUDp	Primary auditory area	0.810	0.639	0.832	0.854	0.727	0.742	0.888	0.870	0.935
19	AUDv	Ventral auditory area	0.759	0.537	0.788	0.803	0.613	0.679	0.842	0.807	0.902
20	PERI	Perirhinal area	0.522	0.373	0.609	0.662	0.390	0.435	0.667	0.704	0.799
21	ECT	Ectorhinal area	0.706	0.539	0.753	0.777	0.565	0.630	0.789	0.812	0.872
22	TEa	Temporal association areas	0.754	0.638	0.829	0.817	0.659	0.663	0.826	0.822	0.898
23	RSPagl	Retrosplenial area, lateral agranular part	0.486	0.641	0.763	0.676	0.673	0.586	0.737	0.723	0.851
24	RSPv	Retrosplenial area, ventral part	0.691	0.789	0.854	0.859	0.784	0.803	0.863	0.840	0.899
25	RSPd	Retrosplenial area, dorsal part	0.543	0.717	0.810	0.780	0.749	0.729	0.810	0.793	0.877
26	VISpm	posteromedial visual area	0.734	0.656	0.848	0.760	0.570	0.612	0.825	0.822	0.863
27	VISp	Primary visual area	0.775	0.852	0.909	0.878	0.839	0.849	0.896	0.892	0.938
28	VISL	Lateral visual area	0.705	0.604	0.815	0.801	0.689	0.765	0.815	0.792	0.882
29	MOB	Main olfactory bulb	0.636	0.849	0.882	0.859	0.441	0.534	0.893	0.909	0.903
30	AOB	Accessory olfactory bulb	0.330	0.523	0.677	0.575	0.005	0.281	0.620	0.677	0.681
31	AON	Anterior olfactory nucleus	0.606	0.748	0.843	0.811	0.391	0.638	0.828	0.871	0.872
32	TT	Taenia tecta	0.364	0.666	0.762	0.777	0.188	0.572	0.777	0.775	0.822
33	DP	Dorsal peduncular area	0.012	0.522	0.748	0.586	0.012	0.474	0.607	0.631	0.768
34	PIR	Piriform area	0.754	0.815	0.870	0.879	0.803	0.790	0.904	0.923	0.938
35	NLOT	Nucleus of the lateral olfactory tract	0.481	0.633	0.747	0.735	0.403	0.693	0.805	0.800	0.886
36	COA	Cortical amygdalar area	0.472	0.810	0.858	0.852	0.764	0.742	0.857	0.849	0.917
37	PAA	Piriform-amygdalar area	0.308	0.730	0.800	0.763	0.705	0.630	0.814	0.825	0.897
38	CA	Ammon''s horn	0.705	0.866	0.874	0.823	0.794	0.822	0.846	0.819	0.913
39	DG	Dentate gyrus	0.589	0.813	0.827	0.752	0.730	0.760	0.770	0.724	0.863

40	ENT	Entorhinal area	0.712	0.851	0.881	0.828	0.794	0.772	0.844	0.840	0.903
41	PAR	Parasubiculum	0.393	0.487	0.566	0.479	0.431	0.539	0.514	0.475	0.656
42	POST	Postsubiculum	0.441	0.696	0.736	0.648	0.616	0.684	0.721	0.702	0.798
43	PRE	Presubiculum	0.429	0.581	0.637	0.474	0.518	0.604	0.545	0.502	0.691
44	SUB	Subiculum	0.374	0.632	0.681	0.531	0.506	0.619	0.555	0.476	0.685
45	CLA	Claustrum	0.312	0.139	0.311	0.459	0.341	0.510	0.636	0.737	0.768
46	EPd	Endopiriform nucleus, dorsal part	0.497	0.397	0.522	0.599	0.478	0.581	0.689	0.789	0.829
47	LA	Lateral amygdalar nucleus	0.412	0.532	0.640	0.622	0.492	0.567	0.700	0.738	0.813
48	BLAa	Basolateral amygdalar nucleus, anterior part	0.547	0.628	0.748	0.735	0.450	0.703	0.767	0.782	0.870
49	BLAp	Basolateral amygdalar nucleus, posterior part	0.527	0.615	0.722	0.680	0.528	0.628	0.707	0.768	0.854
50	BLAv	Basolateral amygdalar nucleus, ventral part	0.458	0.631	0.783	0.709	0.564	0.682	0.732	0.816	0.883
51	BMA	Basomedial amygdalar nucleus	0.573	0.666	0.780	0.767	0.634	0.746	0.789	0.832	0.894
52	PA	Posterior amygdalar nucleus	0.464	0.607	0.675	0.663	0.512	0.550	0.668	0.696	0.811
53	ACB	Nucleus accumbens	0.646	0.723	0.832	0.841	0.569	0.826	0.850	0.857	0.898
54	OT	Olfactory tubercle	0.709	0.777	0.813	0.853	0.670	0.712	0.882	0.889	0.917
55	LSX	Lateral septal complex	0.376	0.798	0.861	0.830	0.611	0.766	0.836	0.831	0.889
56	BA	Bed nucleus of the accessory olfactory tract	0.023	0.488	0.569	0.542	0.195	0.441	0.634	0.508	0.722
57	CEA	Central amygdalar nucleus	0.663	0.662	0.790	0.802	0.649	0.769	0.824	0.827	0.882
58	MEA	Medial amygdalar nucleus	0.629	0.780	0.843	0.828	0.698	0.796	0.850	0.847	0.897
59	IA	Intercalated amygdalar nucleus	0.277	0.350	0.559	0.517	0.189	0.476	0.589	0.583	0.741
60	AAA	Anterior amygdalar area	0.660	0.480	0.701	0.752	0.288	0.704	0.790	0.800	0.864
61	GPe	Globus pallidus, external segment	0.500	0.691	0.786	0.790	0.682	0.683	0.798	0.810	0.868

62	BST	Bed nuclei of the stria terminalis	0.419	0.726	0.785	0.740	0.529	0.700	0.722	0.752	0.823
63	SI	Substantia innominata	0.566	0.518	0.655	0.717	0.422	0.719	0.743	0.778	0.851
64	MA	Magnocellular nucleus	0.573	0.407	0.581	0.646	0.270	0.672	0.675	0.725	0.804
65	NDB	Diagonal band nucleus	0.377	0.554	0.690	0.665	0.345	0.668	0.702	0.695	0.807
66	MS	Medial septal nucleus	0.190	0.557	0.779	0.661	0.400	0.590	0.748	0.700	0.841
67	SPFm	Subparafascicular nucleus, magnocellular part	0.013	0.543	0.618	0.486	0.637	0.428	0.543	0.522	0.661
68	SPFp	Subparafascicular nucleus, parvicellular part	0.368	0.374	0.577	0.574	0.469	0.484	0.554	0.540	0.696
69	SPA	Subparafascicular area	0.063	0.667	0.757	0.562	0.693	0.543	0.559	0.596	0.694
70	MG	Medial geniculate complex	0.668	0.639	0.733	0.671	0.617	0.745	0.735	0.727	0.801
71	LGd	Dorsal part of the lateral geniculate complex	0.598	0.744	0.756	0.695	0.718	0.744	0.729	0.657	0.862
72	PVT	Paraventricular nucleus of the thalamus	0.334	0.724	0.809	0.713	0.605	0.492	0.692	0.695	0.809
73	RE	Nucleus of reuniens	0.375	0.632	0.732	0.580	0.615	0.557	0.573	0.616	0.807
74	RH	Rhomboid nucleus	0.251	0.375	0.568	0.313	0.549	0.454	0.352	0.399	0.602
75	CM	Central medial nucleus of the thalamus	0.235	0.569	0.620	0.556	0.376	0.359	0.598	0.615	0.688
76	CL	Central lateral nucleus of the thalamus	0.464	0.420	0.681	0.544	0.633	0.584	0.542	0.606	0.663
77	PF	Parafascicular nucleus	0.286	0.600	0.799	0.646	0.701	0.638	0.653	0.685	0.771
78	IMD	Intermediodorsal nucleus of the thalamus	0.400	0.505	0.714	0.564	0.672	0.541	0.594	0.657	0.740
79	MD	Mediodorsal nucleus of thalamus	0.573	0.744	0.881	0.770	0.814	0.765	0.776	0.808	0.865
80	SMT	Submedial nucleus of the thalamus	0.304	0.562	0.737	0.529	0.638	0.556	0.557	0.576	0.720
81	LP	Lateral posterior nucleus of the thalamus	0.583	0.705	0.762	0.707	0.687	0.732	0.699	0.741	0.838
82	AV	Anteroventral nucleus of thalamus	0.417	0.677	0.803	0.759	0.627	0.622	0.752	0.757	0.812
83	AM	Anteromedial nucleus	0.358	0.674	0.846	0.732	0.673	0.613	0.701	0.705	0.819

84	LPO	Lateral preoptic area	0.336	0.512	0.636	0.646	0.425	0.634	0.637	0.696	0.804
85	LHA	Lateral hypothalamic area	0.561	0.735	0.818	0.770	0.756	0.812	0.784	0.847	0.890
86	RCH	Retrochiasmatic area	0.117	0.504	0.541	0.524	0.459	0.432	0.507	0.534	0.706
87	TU	Tuberal nucleus	0.142	0.716	0.756	0.675	0.711	0.703	0.722	0.754	0.828
88	ZI	Zona incerta	0.571	0.674	0.755	0.712	0.701	0.669	0.720	0.748	0.830
89	AHN	Anterior hypothalamic nucleus	0.314	0.630	0.723	0.706	0.645	0.657	0.682	0.756	0.825
90	MPN	Medial preoptic nucleus	0.191	0.635	0.747	0.680	0.458	0.597	0.664	0.645	0.820
91	VMH	Ventromedial hypothalamic nucleus	0.317	0.743	0.774	0.616	0.781	0.746	0.674	0.759	0.844
92	DMH	Dorsomedial nucleus of the hypothalamus	0.302	0.651	0.778	0.576	0.696	0.624	0.582	0.712	0.808
93	SBPV	Subparaventricular zone	0.151	0.454	0.548	0.439	0.444	0.386	0.461	0.427	0.620
94	PVH	Paraventricular hypothalamic nucleus	0.303	0.584	0.632	0.463	0.501	0.393	0.481	0.562	0.762
95	ARH	Arcuate hypothalamic nucleus	0.070	0.720	0.727	0.576	0.711	0.625	0.618	0.605	0.787
96	SCs	Superior colliculus, sensory related	0.340	0.678	0.754	0.745	0.586	0.704	0.756	0.788	0.800
97	IC	Inferior colliculus	0.565	0.827	0.833	0.733	0.768	0.809	0.742	0.721	0.889
98	NB	Nucleus of the brachium of the inferior colliculus	0.292	0.538	0.599	0.378	0.399	0.492	0.505	0.561	0.643
99	CUN	Cuneiform nucleus	0.437	0.698	0.799	0.620	0.563	0.675	0.595	0.604	0.793
100	RR	Midbrain reticular nucleus, retrorubral area	0.454	0.582	0.644	0.637	0.588	0.622	0.669	0.647	0.770
101	MRN	Midbrain reticular nucleus	0.744	0.775	0.847	0.815	0.785	0.792	0.817	0.838	0.882
102	PAG	Periaqueductal gray	0.715	0.839	0.881	0.824	0.817	0.825	0.818	0.846	0.908
103	VTA	Ventral tegmental area	0.280	0.668	0.696	0.692	0.702	0.665	0.760	0.709	0.816
104	SNr	Substantia nigra, reticular part	0.531	0.773	0.815	0.782	0.761	0.772	0.812	0.789	0.877
105	RN	Red nucleus	0.697	0.804	0.851	0.832	0.804	0.797	0.844	0.859	0.885

106	APN	Anterior pretectal nucleus	0.631	0.771	0.851	0.786	0.786	0.824	0.792	0.800	0.864
107	PPT	Posterior pretectal nucleus	0.083	0.345	0.517	0.458	0.253	0.404	0.484	0.498	0.628
108	SNc	Substantia nigra, compact part	0.133	0.370	0.460	0.375	0.442	0.460	0.495	0.472	0.670
109	PPN	Pedunculopontine nucleus	0.707	0.748	0.842	0.798	0.759	0.753	0.779	0.772	0.867
110	IPN	Interpeduncular nucleus	0.420	0.775	0.810	0.772	0.706	0.680	0.820	0.832	0.863
111	CLI	Central linear nucleus raphe	0.263	0.679	0.702	0.688	0.642	0.617	0.707	0.711	0.803
112	DR	Dorsal nucleus raphe	0.553	0.691	0.767	0.669	0.574	0.615	0.605	0.673	0.772
113	NLL	Nucleus of the lateral lemniscus	0.444	0.654	0.752	0.676	0.626	0.641	0.696	0.671	0.787
114	PSV	Principal sensory nucleus of the trigeminal	0.481	0.727	0.811	0.753	0.751	0.768	0.770	0.766	0.843
115	PB	Parabrachial nucleus	0.490	0.706	0.793	0.675	0.614	0.662	0.661	0.618	0.815
116	V	Motor nucleus of trigeminal	0.622	0.629	0.788	0.708	0.749	0.768	0.750	0.757	0.841
117	PRNc	Pontine reticular nucleus, caudal part	0.716	0.705	0.835	0.776	0.823	0.803	0.847	0.884	0.893
118	PCG	Pontine central gray	0.402	0.627	0.707	0.611	0.491	0.564	0.598	0.603	0.756
119	B	Barrington''s nucleus	0.141	0.415	0.614	0.316	0.181	0.281	0.228	0.315	0.614
120	CS	Superior central nucleus raphe	0.669	0.700	0.812	0.768	0.757	0.741	0.835	0.854	0.887
121	LDT	Laterodorsal tegmental nucleus	0.362	0.618	0.729	0.565	0.554	0.591	0.550	0.521	0.759
122	NI	Nucleus incertus	0.467	0.502	0.612	0.527	0.384	0.558	0.643	0.726	0.782
123	RPO	Nucleus raphe pontis	0.617	0.567	0.650	0.609	0.593	0.641	0.717	0.701	0.776
124	PG	Pontine gray	0.555	0.813	0.822	0.743	0.679	0.707	0.792	0.782	0.835
125	TRN	Tegmental reticular nucleus	0.487	0.687	0.729	0.600	0.586	0.587	0.679	0.756	0.795
126	PRNr	Pontine reticular nucleus	0.748	0.765	0.871	0.830	0.822	0.814	0.862	0.890	0.912
127	CN	Cochlear nuclei	0.614	0.781	0.800	0.753	0.691	0.676	0.748	0.725	0.833

128	DCN	Dorsal column nuclei	0.654	0.362	0.780	0.682	0.302	0.045	0.748	0.727	0.826
129	ECU	External cuneate nucleus	0.353	0.492	0.598	0.590	0.338	0.001	0.640	0.615	0.746
130	NTB	Nucleus of the trapezoid body	0.284	0.587	0.630	0.543	0.666	0.509	0.666	0.751	0.699
131	NTS	Nucleus of the solitary tract	0.557	0.502	0.740	0.640	0.533	0.156	0.693	0.651	0.814
132	GRN	Gigantocellular reticular nucleus	0.766	0.672	0.815	0.813	0.814	0.658	0.842	0.860	0.890
133	IRN	Intermediate reticular nucleus	0.730	0.532	0.777	0.746	0.755	0.622	0.810	0.816	0.872
134	PARN	Parvicellular reticular nucleus	0.677	0.502	0.775	0.718	0.785	0.624	0.804	0.805	0.860
135	MDRN	Medullary reticular nucleus	0.807	0.495	0.811	0.773	0.514	0.148	0.862	0.855	0.887
136	IO	Inferior olivary complex	0.407	0.542	0.697	0.609	0.554	0.188	0.625	0.647	0.776
137	LRN	Lateral reticular nucleus	0.522	0.538	0.735	0.702	0.490	0.043	0.736	0.701	0.818
138	MV	Medial vestibular nucleus	0.740	0.817	0.892	0.828	0.759	0.691	0.837	0.820	0.893
139	VERM	Vermal regions	0.727	0.896	0.904	0.839	0.777	0.661	0.838	0.818	0.905
140	HEM	Hemispheric regions	0.721	0.900	0.904	0.858	0.782	0.565	0.835	0.832	0.902

Supplementary Table 8 Mean Dice Scores of different methods and P values of Wilcoxon signed-rank test among DeepMapi and other methods.

Methods		Mean dice scores	P values
Traditional methods	Affine	0.493 ± 0.219	3.109e-116
	LD Deomons	0.637 ± 0.179	1.171e-111
	SyN	0.756 ± 0.127	2.217e-68
Unsupervised methods	VoxelMorph	0.698 ± 0.154	3.244e-112
	AVSM	0.582 ± 0.200	5.869e-113
	RDMM	0.623 ± 0.185	1.680e-112
	QuickSilver	0.728 ± 0.152	5.460e-92
Supervised methods	VNet	0.740 ± 0.151	2.382e-84
	DeepMapi	0.826 ± 0.091	—

Supplementary Table 9 The comparison of self-feedback strategy with smaller step size, including the mean Dice Scores, P values and training time.

Sample strategy	Mean dice scores	P values	Training time approximate (days)
Self-feedback	0.822 ± 0.101	—	~ 2
32 stride	0.813 ± 0.101	9.8912e-13	~ 4
28 stride	0.811 ± 0.102	1.9425e-09	~ 5
24 stride	0.816 ± 0.099	3.1239e-06	~ 8
20 stride	0.816 ± 0.100	1.5159e-04	~ 12
16 stride	0.819 ± 0.096	0.019	~ 21